

Proteomic Analysis of Interaction between a Plant Virus and Its Vector Insect Reveals New Functions of Hemipteran Cuticular Protein*[§]

Wenwen Liu[‡], Stewart Gray[§], Yan Huo[¶], Li Li[‡], Taiyun Wei, and Xifeng Wang^{‡**}

Numerous viruses can be transmitted by their corresponding vector insects; however, the molecular mechanisms enabling virus transmission by vector insects have been poorly understood, especially the identity of vector components interacting with the virus. Here, we used the yeast two-hybrid system to study proteomic interactions of a plant virus (*Rice stripe virus*, RSV, genus *Tenuivirus*) with its vector insect, small brown planthopper (*Laodelphax striatellus*). Sixty-six proteins of *L. striatellus* that interacted with the nucleocapsid protein (pc3) of RSV were identified. A virus–insect interaction network, constructed for pc3 and 29 protein homologs of *Drosophila melanogaster*, suggested that nine proteins might directly interact with pc3. Of the 66 proteins, five (atlasin, a novel cuticular protein, jagunal, NAC domain protein, and vitellogenin) were most likely to be involved in viral movement, replication, and transovarial transmission. This work also provides evidence that the novel cuticular protein, CPR1, from *L. striatellus* is essential for RSV transmission by its vector insect. CPR1 binds the nucleocapsid protein (pc3) of RSV both *in vivo* and *in vitro* and colocalizes with RSV in the hemocytes of *L. striatellus*. Knockdown of CPR1 transcription using RNA interference resulted in a decrease in the concentration of RSV in the hemolymph, salivary glands and in viral transmission efficiency. These data suggest that CPR1 binds RSV in the insect and stabilizes the viral concentration in the hemolymph, perhaps to protect the virus or to help move the virus to the salivary tissues. Our studies provide direct experimental evidence that viruses can use existing vector proteins to aid their survival in the hemolymph. Identifying these pu-

tative vector molecules should lead to a better understanding of the interactions between viruses and vector insects. *Molecular & Cellular Proteomics* 14: 10.1074/mcp.M114.046763, 2229–2242, 2015.

Most plant viruses depend on specific vectors for transmission among host plants with insects, especially hemipteran insects with piercing-sucking mouthparts, the most common vectors (1, 2). Transmission by insect vectors is a complex process involving specific interactions between the virus, the vector, and the host plant, and these interactions are further influenced by environmental conditions. Four distinct transmission mechanisms have been described for vector-borne plant viruses: nonpersistent, stylet-borne; semipersistent, foregut-borne; persistent, circulative, nonpropagative; and persistent, circulative, propagative (2, 3). Once acquired, persistent, circulative, propagative viruses are retained for the life of the insect vectors, and they can replicate in various insect tissues. Thus, these viruses can be regarded as both plant and insect viruses (4, 5). After the insect ingests the virus during feeding, the virus moves through the alimentary canal of the insect, infects the gut epithelial cells, and then is released into the hemolymph where it can spread to other tissues and organs. Ultimately, the virus infects the salivary glands and is released into the salivary ducts where it can be transferred to new plants via the saliva released during feeding (3). The success and efficiency of virus transmission requires specific interactions between the virus and unknown components of the vector to allow transport of the virus in and out of insect tissues and to overcome the various types of insect immune reactions (4, 6, 7). The viral components involved in the virus–vector interactions are relatively well established for several circulative viruses (8, 9). In contrast, the components of the insect vector that participate in viral transmission have been difficult to study, although some insect proteins have been identified that interact with circulative viruses and are linked to successful transmission (10–13). Insect proteins are expected to play a role as virus receptors, in the uptake and transport of virus through various tissues, and in replication of the viruses (1, 3, 14). In our recent study, vitellogenin of *Laodelphax striatellus* (small brown planthopper) was demonstrated to play a critical role in transovarial

From the [‡]State Key Laboratory for Biology of Plant Diseases and Insect Pests, Institute of Plant Protection, Chinese Academy of Agricultural Sciences, Beijing 100193, China; [§]USDA, ARS, Plant Protection Research Unit, Cornell University, Ithaca, NY; [¶]State Key Laboratory of Plant Genomics, Institute of Microbiology, Chinese Academy of Sciences, Beijing 100080, China; Fujian Province Key Laboratory of Plant Virology, Institute of Plant Virology, Fujian Agriculture and Forestry University, Fuzhou 350002, China

Received November 26, 2014, and in revised form, March 30, 2015
Published, MCP Papers in Press June 19, 2015, DOI 10.1074/mcp.M114.046763

Author contributions: W.L. and X.W. designed the research; W.L., Y.H., L.L., and X.W. performed the research; W.L., S.G., T.W., and X.W. analyzed the data; and W.L., S.G., T.W., and X.W. wrote the paper.

transmission of *Rice stripe virus* (RSV) (15). Diverse proteins of *Sogatella furcifera* (white-backed planthopper) have also been identified as acting in the successful transmission of southern rice black-streaked dwarf virus (16).

Additionally, insects have a well-developed innate immune system that relies on humoral and cellular responses (17). Humoral immune responses include the synthesis of antimicrobial peptides and triggering of enzymatic cascades that regulate coagulation, melanization of foreign material in the hemolymph, and the production of reactive oxygen and nitrogen species (18). Cellular-mediated immune responses include phagocytosis, nodulation and encapsulation, and melanization (19). For successful survival, movement, and/or replication in vector insects, the virus needs to avoid the immune responses of the insect. Circulative plant viruses spend considerable time in the insect hemocoel (5), suggesting that these viruses have developed or adapted methods to escape the insect immune responses. In circulative, non-propagative viruses, the protein GroEL, secreted by endosymbiotic bacteria of aphids and whiteflies, can bind to the viruses and may act to protect the virus from rapid degradation in the hemolymph (20), although a recent study has called into question this mechanism in aphids (21). Multiple mechanisms or proteins likely act to help circulative viruses remain viable in the hemolymph of insects.

RSV, a member of the genus *Tenuivirus*, is responsible for significant yield losses in rice production in temperate and subtropical East Asia (22). RSV has filamentous ribonucleo-protein particles (RNPs) that contain four single-stranded RNAs that encode seven proteins. The ambisense RNA3 encodes two proteins, the silencing suppressor p3 (23.9 kDa) and the nucleocapsid protein pc3 (35 kDa) (22, 23). RSV is transmitted in a circulative, persistent, propagative manner by the small brown planthopper (*L. striatellus*). High densities of this insect can damage cereal crops in the field directly by feeding, but low densities of RSV-infected insects can result in even greater yield losses by transmitting RSV (24).

Here, we took advantage of several molecular biological tools, including the yeast two-hybrid assay, immunofluorescence, and RNA interference induced by synthesized dsRNA, to investigate the molecular mechanisms of RSV transmission by its vector insect (*L. striatellus*). Numerous proteins from *L. striatellus* were found to interact with RSV pc3, and four proteins were proposed to be involved in viral movement, replication, or transovarial transmission. Further, we have provided direct experimental evidence that a hemipteran cuticular protein is involved in virus transmission.

EXPERIMENTAL PROCEDURES

Insect Rearing—Nonviruliferous and viruliferous *L. striatellus* were reared on healthy and RSV-infected rice seedlings (cv. Wuyujing 3), respectively. The insects were transferred to fresh seedlings each week (25). To ensure the virus was maintained in the insects that fed on virus-infected plants, we periodically collected offspring from an individual female and tested for the presence of RSV using RT-PCR.

Yeast Two-Hybrid Assay—The yeast two-hybrid system can detect protein–protein interactions in the living cells. Here, we adopted the system based on split-ubiquitin provided by the DUALhunter starter kit (Dualsystems Biotech, Zurich, Switzerland) to study the interactions of RSV pc3 with those of its vector insect. A cDNA library of *L. striatellus* was constructed in the prey plasmid, SfiI-digested pPR3-N, using the EasyClone cDNA library construction kit (Dualsystems Biotech). The ligation plasmid was transferred into competent cells of *Escherichia coli* strain DH10B by electroporation. The titer of the primary cDNA library was calculated using the number of clones on plates. Colony PCR was used to confirm the size of the inserted fragments in the library. The bait plasmid was constructed by cloning the full-length RSV pc3 gene into pDHB1 using specifically designed primers (Table S1). The recombinant plasmid pDHB1-pc3 was used to transform yeast strain NMY51 then selected on synthetic defined minimal medium lacking leucine (S.D./-Leu). The expression of RSV pc3 in the yeast was confirmed by Western blotting and functional assays. Finally, the bait plasmid pDHB1-pc3 and the cDNA library of *L. striatellus* were used to cotransform yeast strain NMY51. Positive clones were selected on the triple dropout medium (triple dropout medium: S.D./-His/-Leu/-Trp) with 3-aminotriazole (3-AT). Then the clones were restreaked on quadruple dropout medium (QDO: S.D./-Ade/-His/-Leu/-Trp) with 3-AT. For distinguishing false-positive interactions, the plasmids encoding the interacting proteins were used to cotransform yeast strain NMY51, and β -galactosidase activity was detected using the HTX high-throughput β -galactosidase kit (Dualsystems Biotech). Plasmids from the positive clones were recovered, used to transform *E. coli* strain DH5 α , and sequenced to identify putative insect proteins that interacted with RSV pc3. All sequences were assembled by the SeqMan II program (DNASTar) to remove the repetitive sequences. The different sequences were used in a BLAST search of the NCBI database (<http://blast.st-va.ncbi.nlm.nih.gov/Blast.cgi>). Gene Ontology (GO) annotations of molecular function were assigned according to the Blast2go database (<http://www.blast2go.com>). These proteins were determined using the ortholog annotation from *D. melanogaster* in FlyBase (<http://flybase.org/>). Network diagrams were created using the database Search Tool for the Retrieval of Interacting Genes/Proteins (STRING 9.1; <http://string-db.org>), with a parameter setting confidence score of autodetect organism for any clusters of orthologous groups of proteins (26).

Chemiluminescent Co-IP Assay—The DNA sequences of RSV pc3 and prey proteins were cloned into the mammalian expression vector pAcGFP1, which encodes GFP, and pProLabel, which encodes the ProLabel tag, using the designed primers in Table S1. The recombinant plasmids were cotransfected into human embryonic kidney 293FT cells with FuGENE HD (Roche, Basel, Switzerland). After 36 h, the number of transfected cells was estimated by visualizing green fluorescence of GFP to confirm pAcGFP1-pc3 expression. Interacting proteins were then immunoprecipitated with the Matchmaker chemiluminescent Co-IP kit according to the manufacturer's protocol (Clontech, San Francisco, CA). Briefly, cells were washed with 37 °C-preheated PBS and digested with 0.01% trypsin for 3 min. Preheated medium (DMEM + 10% FBS) was added to terminate trypsin digestion, the cell precipitate was washed twice with PBS and 500 μ l cell lysis buffer added. The concentration of total protein was determined with a BCA protein assay kit (Pierce, Rockford), then 250 μ g of each lysate were transferred to a new tube and the volume increased to 500 μ l using cold cell lysis buffer. One microliter of AcGFP polyclonal antibody was added and the mixture incubated at 4 °C for 2 h. Washed agarose beads (25 μ l) were then added, and the mixture was incubated at 4 °C overnight with continual rotation. The beads were collected by gentle centrifugation and washed five times with wash buffer 1 then four times with wash buffer 2. Protein–protein interactions were determined by ProLabel detection of the beads. Each

sample of beads was resuspended in 80 μ l lysis buffer and transferred to a well in a 96-well assay plate. To each well, 30 μ l of substrate mix were added, then ProLabel activity was measured using Monolight by GloMax 96 Microplate Luminometer (Promega, Madison, WI).

Full-Length Amplification of the CPR1 Gene, Protein Expression, and Antibody Production—The sequence of the CPR1 fragment identified from the yeast two-hybrid experiment was used to design primers (Table S1) to amplify the full-length gene sequence directly from total RNA extracted from *L. striatellus* using the standard Trizol reagent protocol (Invitrogen, Carlsbad, CA). Full-length CPR1 cDNA was subsequently acquired using a 5' RACE System for Rapid Amplification of cDNA Ends Kit (Invitrogen). The CPR1 gene was cloned into the prokaryotic expression vector, pDEST17, which was then used to transform *E. coli* strain Rosetta. The recombinant plasmid pDEST17-CPR1 in Rosetta was expressed by adding isopropyl β -D-1-thiogalactopyranoside. The expressed protein CPR1 was purified with Ni-NTA resin (Qiagen, Chatsworth, CA) and used to immunize rabbits to obtain a CPR1-specific polyclonal antibody (27). IgG was isolated from specific polyclonal antisera using a protein A-Sepharose affinity column (Sigma, St. Louis, MO). The specificity of the anti-CPR1 antibody was analyzed in a Western blot against total proteins extracted from *L. striatellus*. An RSV monoclonal antibody was kindly provided by Xueping Zhou (Zhejiang University).

Sequence Alignments and Phylogenetic Analysis—The amino acid sequences for 25 cuticular proteins from various insects were obtained from GenBank and aligned with the CPR1 sequence initially using the MUSCLE algorithm (28). All sequence alignments were adjusted by visual inspection to ensure that the alignments were biologically relevant (29). Phylogenetic reconstructions for a NJ tree were obtained using the neighbor-joining method and the WAG+G+I+F amino acid substitution model implemented in the MEGA v.5 program (30). Support for the internal nodes of the trees was evaluated by the bootstrap method with 10,000 pseudo-replicates (31). Nodes with bootstrap support <40% were collapsed to the nearest significant node.

GST Pull-Down Assay—The gene of CPR1 (1aa-215aa), CPR1N (1aa-90aa), and CPR1C (91aa-215aa) were amplified and cloned into pET28a for fusion with his-tag. RSV pc3 cDNA fragments were amplified and cloned into pGEX-3X for fusion with glutathione S-transferase (GST)¹. All recombinant proteins were expressed in *E. coli* strain BL21. The GST-tag fused protein, RSV pc3-GST, was bound to glutathione-Sepharose beads for 3 h at 4 °C. The mixtures were centrifuged for 5 min at 100 \times g. The his-tag fusion proteins were added to the beads and incubated for 2 h at 4 °C. After being centrifuged and washed five times with wash buffer (300 mM NaCl, 10 mM Na₂HPO₃, 2.7 mM KCl, and 1.7 M KH₂PO₄) at 4 °C, the bead-bound proteins were separated by SDS-PAGE gel electrophoresis and detected by Western blotting with his-tag antibodies.

Construction of Baculovirus Plasmids and the Transfection of Spodoptera frugiperda 9 Cells—The CPR1 and RSV pc3 genes amplified with the designed primers (Table S1) were inserted into pDEST8 plasmids and into *E. coli* DH10Bac cells for transposition into the bacmid, respectively. The recombinant bacmid was isolated and

used to transfect *S. frugiperda* (Sf9) cells in the presence of Cell FECTIN according to the instructions (Invitrogen). For cytological observations, Sf9 cells were cultured on cover slips and further incubated at 27 °C for 72 h. The supernatant collected from the transfected Sf9 cell culture was transferred again to fresh Sf9 cells before being processed for immunofluorescence microscopy described later.

Culture of L. striatellus Cell Line—The *L. striatellus* cell line was established by adapting the protocol already detailed (32). Nonviruliferous eggs of *L. striatellus* that had been oviposited 8 days earlier in leaf sheaths of rice plants were surface-sterilized with 70% ethanol, and embryonic fragments were dissected from the eggs in Tyrode's solution, treated with 0.25% trypsin in Tyrode's solution for 15 min, and then incubated with Kimura's insect medium at 25 °C. The medium was changed every 7–10 days. RSV inoculum was prepared from infected plants that were surface sterilized with 70% ethanol. The sterilized leaves were ground in a solution of 0.1 M histidine that contained 0.01 M MgCl₂, pH 6.2 (His-Mg) and centrifuged. The supernatant was used to inoculate cell monolayers of *L. striatellus* after 30 passages of culture. The cells were washed twice with His-Mg and covered with Kimura's insect medium after 2 h then cultured to confluence in the culture flasks and subcultured at intervals of 10 days through 10 passages.

Isolation of Insect Hemocytes—Glass cover slips (12 mm diameter) were soaked in alkaline wash solution (10% w/v NaOH + 60% v/v ethanol) in a single layer without overlapping for 2 h and washed five times with distilled water. The cover slips were then treated with anhydrous ethanol for 30 min and immediately dried over an alcohol lamp. After incubating in 0.1 mg/ml poly (L-lysine) for 2 h, the treated cover slips were washed three times with distilled water and dried at room temperature for at least 3 days before use (33). Individual insects were held on ice in a glass dish, a leg was removed, and a drop of hemolymph was collected from the leg wound (34). The hemolymph was incubated on the poly (L-lysine)-coated cover slips for 45 min at 30 °C to allow adhesion of hemocytes, then the cover slips were washed four times to remove unattached cells.

Immunofluorescence Assay—CPR1 and RSV antibodies were conjugated, respectively, with Alexa Fluor 594 (red) and Alexa Fluor 488 (green) using the manufacturer's protocol (Invitrogen). Sf9 cells or hemocytes previously fixed on the cover slips were incubated in 2% paraformaldehyde diluted in water for 30 min at room temperature. Various excised tissues of *L. striatellus* were incubated in 2% paraformaldehyde for 1 h. After washing with phosphate-buffered saline (PBS), cells or tissues were incubated in osmotic buffer (1% Triton X-100 in PBS) for 2 h and washed three times in PBS (35). The treated cells or tissues were then incubated with labeled antibody for 2 h at 37 °C, washed three times with PBS, and visualized by confocal microscopy (TCS SP5, Leica, Wetzlar, Germany).

Real-Time Quantitative RT-PCR (qRT-PCR) Analysis—The total RNA of viruliferous *L. striatellus* was extracted using Trizol reagent according to the manufacturer's instructions. The cDNA was synthesized from 1 μ g RNA using a Fast Quant RT Kit (TIANGEN, Beijing, China). The percentage efficiency of primers (Table S1) was determined from standard curves for genes of CPR1, pc3, and actin (internal reference gene). First, five 10-fold serial dilutions of cDNA for each gene in duplicate were amplified by real-time qRT-PCR in a final volume of 20 μ l using a Super Real PreMix Plus (SYBR Green) Kit (TIANGEN) and an iQ5 real-time PCR system (Bio-Rad, Hercules, CA). These data were then used for relative quantification using the 2^{- $\Delta\Delta$ ct} method, which confines all the controls as one.

RNA Interference in L. striatellus—For synthesizing dsRNA, first, the full-length sequences of CPR1 and GFP were amplified by PCR using gene-specific primers with 23 bases of the T7 RNA polymerase promoter added according to the protocol of the T7 RiboMAX

¹ The abbreviations used are: aa, amino acid; bp, base pair; Co-IP, co-immunoprecipitation assay; CPR1, a novel cuticular protein with RR1 consensus; GST, glutathione s-transferase; kDa, kilodalton; *L. striatellus*, small brown planthopper (*Laodelphax striatellus*); PBS, phosphate-buffered saline; PCR, polymerase chain reaction; RACE, rapid amplification of cDNA ends; RNAi, RNA interference; RSV, *Rice stripe virus*; RSV pc3, nucleocapsid protein of *Rice stripe virus*; RSV RNPs, filamentous ribonucleoprotein particles of *Rice stripe virus*; RT-PCR, reverse transcription-polymerase chain reaction.

ExpressRNAi System (Promega) (Table S1). The PCR products were then used as templates for dsRNA synthesis using the same system. After synthesis, the dsRNA was purified by isopropanol precipitation. Its purity and integrity were assessed by agarose gel electrophoresis. According to the method for the brown planthopper (36), the third-instar viruliferous nymphs of *L. striatellus* were each injected with 23 nl CPR1 dsRNA (3 $\mu\text{g}/\mu\text{l}$) or with GFP dsRNA (3 $\mu\text{g}/\mu\text{l}$) as a control using an Auto-Nanoliter Injector (Drummond, Broomall, PA). The injected insects were transferred to fresh rice seedlings in culture beakers then removed at different times to test for expression of CPR1 and pc3. For testing for CPR1 and pc3 expression, the salivary gland and gut were excised separately for bulk analysis by organ type and hemolymph collected from 20 insects to extract RNA for analysis of the CPR1 and pc3 transcript levels using real-time qRT-PCR at each sampling (37).

To determine the effects of CPR1 silencing on transmission efficiency, 50 viruliferous *L. striatellus* were injected with dsRNA of CPR1 and GFP, then allowed to feed on healthy rice seedlings for 6 days. Insects were transferred to healthy rice seedlings (1/plant) for a 2-h inoculation access period, and the seedlings were then grown in a greenhouse for 2 weeks. The infection status of each seedling was assessed using specific primers for RSV pc3 by RT-PCR (Table S1). The entire RNA interference experiment was repeated three times.

RESULTS

Isolation and Analysis of Proteins in *L. striatellus* That Interact with RSV pc3—The workflow to obtain the proteins of *L. striatellus* that interact with RSV pc3 using the yeast two-hybrid technique is detailed in Fig. S1A. The titer of the primary cDNA library of *L. striatellus* constructed was 1.2×10^6 cfu/19.5 μl with an average insert size of 1.5 kb, meeting the requirements of a standard cDNA library (Fig. S1B). The bait pDHB1-pc3 was correctly expressed in yeast as verified using an anti-LexA monoclonal antibody in a Western blot analysis (Fig. S1C). The bait fusion protein was determined to be functionally well expressed in the assay without nonspecific background by cotransforming the pDHB1-pc3 plasmid with the positive control prey plasmid pOst1-Nubl and negative plasmid pPR3-N to test expression in a functional assay. Co-expression of pDHB1-pc3 with pOst1-Nubl in the yeast resulted in reporter gene activation as seen by growth on all selective medium, whereas the bait protein coexpressed with the NubG-nonsense peptide fusion plasmid pPR3-N did not grow on the selective medium (Fig. S1D). The library screen background was reduced by growing pDHB1-pc3 and empty library vector pPR3-N on triple dropout medium supplemented with different concentrations of 3-AT; there was no background growth on 20 mM 3-AT, so it was used for the library screen. Finally, more than 300 positive clones were isolated by this library screen. After sequencing, these positive clones were found to encode 111 unique proteins.

Of these proteins, 66 proteins were identified by their similarity to available reference sequences in a BLAST search of the NCBI database (Table I). No information could be determined for the remaining 45 putative proteins because the genome of *L. striatellus* has not been sequenced and the protein sequences did not match any insect proteins in the

database. The species distribution of the best matches for each sequence is shown in Fig. 1A. Ten proteins had the highest match with *Acyrtosiphon pisum*, followed by seven proteins with *Tribolium castaneum*, five proteins with *L. striatellus*, and four proteins with *Culex quinquefasciatus* (Fig. 1A). According to the GO annotation analysis, these proteins were assigned to 12 molecular function groups: nine with hydrolase activity, eight with oxidoreductase activity, eight with proteinase activity, seven structural molecules, seven with transporter activity, six with small molecule binding activity, five with protein binding activity, five with transferase activity, four with ion binding activity, four with nucleic acid binding activity, two with lipid binding activity, one with carbohydrate binding activity (Fig. 1B). For generating a protein network for the described interacting proteins, these sequences were used in a search for homology against proteins of *D. melanogaster*. Of the 66 candidates, homologs for 34 proteins were found, and 29 of these proteins and RSV pc3 were in the protein interaction network. In this protein network, RSV pc3 interacted with nine proteins that belong to different groups, *i.e.* structural molecule, ubiquitin, nucleic acid binding, transport and membrane protein group (Fig. 2). This virus–insect interaction network was further supported by the yeast two-hybrid assay results that showed RSV pc3 might interact with various vector insect proteins with different functions. This protein interaction network provided a new insight into the molecular basis of virus transmission by vector insect.

Confirmation of the Interaction Between the Proteins of *L. striatellus* and pc3 of RSV—To confirm a true interaction between RSV pc3 and any of the prey proteins, we selected 12 proteins (ribosome associated membrane protein, NAC domain protein, calcium-transporting ATPase, synaptic vesicle protein, selenoprotein T, jagunal, G-protein coupled receptor, ribosomal protein L13e, vitellogenin, 40S ribosomal protein S28, atlastin, and cuticular protein) that represented different molecular functions for further analysis with the yeast two-hybrid system. These prey plasmids and bait plasmid pDHB1-pc3 were used to cotransform yeast. The yeast clones were cultured on quadruple dropout medium (SD/-Leu/-Trp/-His/-Ade) then analyzed with the β -galactosidase assay. All 12 proteins were confirmed to interact with RSV pc3 in yeast (Fig. S2).

Among the examined interactors from the yeast two-hybrid analysis, five proteins (atlastin, cuticular protein, jagunal, NAC domain protein, and vitellogenin) that are likely associated with viral movement, replication, or transmission were confirmed to interact with RSV pc3 in 293 FT human embryonic kidney cells using a chemiluminescent co-immunoprecipitation (Co-IP) assay. Each protein was coexpressed with RSV pc3 in the 293FT cells. RSV pc3 fused with GFP and the prey proteins tagged with the Prolabel were all well expressed in the cells (Figs. 3A and 3B). In the Co-IP analysis, the relative strength of the interaction between RSV pc3 and five proteins was in order from high to low: cuticular protein (CPR1)

TABLE I

BLAST search of NCBI database for putative proteins of *Laodelphax striatellus* that interacted with the nucleocapsid protein pc3 of RSV in the yeast two-hybrid assay

No.	Accession	Protein	Species	Total score	Coverage (%)	E-value	Identity (%)
1	AAV84265	Ubiquitin	<i>Culicoides sonorensis</i>	520	68	3e-79	98
2	XP_967899	Similar to ribosomal protein L13e	<i>Tribolium castaneum</i>	93.6	78	5e-21	57
3	BAD27585	Capsid protein precursor	<i>Himantobius P virus</i>	622	91	0	97
4	XP_966498	Similar to VAMP-associated protein	<i>Tribolium castaneum</i>	189	54	2e-54	52
5	KC485263	Cuticular protein RR family	<i>Laodelphax striatellus</i>	1,197	100	0	100
6	XM_001950574	Coronin-1C-like	<i>Acyrtosiphon pisum</i>	60.8	4	5e-05	73
7	EU035822	40S ribosomal protein S28-like protein	<i>Phlebotomus papatasi</i>	203	54	1e-48	82
8	YP_003359328	Cytochrome c oxidase subunit II	<i>Laodelphax striatellus</i>	264	69	3e-67	100
9	YP_003359331	Cytochrome c oxidase subunit III	<i>Laodelphax striatellus</i>	184	71	2e-38	99
10	NP_001119674	Fatty acid desaturase	<i>Acyrtosiphon pisum</i>	469	57	2e-158	69
11	ZP_04850405	Conserved hypothetical protein	<i>Bacteroides</i>	36.2	70	3.5	22
12	AFJ86438	Cytochrome P450 CYP6ER2	<i>Laodelphax striatellus</i>	352	89	4e-118	97
13	NP_001155374	Cytochrome b reductase 1-like	<i>Acyrtosiphon pisum</i>	39.3	7	1.6	63
14	KC740896	CsCYTB5 cytochrome B5	<i>Coptotermes formosanus</i>	141	12	3e-29	70
15	XP_001862645	Short-chain dehydrogenase	<i>Culex quinquefasciatus</i>	216	69	7e-66	58
16	YP_004891565	NADH dehydrogenase subunit 2	<i>Phalera flavescens</i>	30	63	9.5	48
17	ZP_03046466	AatD, apolipoprotein N-acyltransferase	<i>Escherichia coli</i>	37.4	52	1.6	26
18	XP_975007	Glycerol-3-phosphate dehydrogenase	<i>Tribolium castaneum</i>	270	43	1e-83	83
19	NP_001040134	Isocitrate dehydrogenase	<i>Bombyx mori</i>	494	85	2e-153	75
20	YP_802425	3-dehydroquinate synthase	<i>Candidatus carsonella ruddii</i>	38.5	93	0.61	26
21	ABN11966	Putative acyl-coenzyme a dehydrogenase	<i>Maconellicoccus hirsutus</i>	132	34	3e-34	94
22	NP_001119645	ATP synthase subunit beta	<i>Acyrtosiphon pisum</i>	132	33	4e-33	97
23	EFX71334	Cytosolic malate dehydrogenase	<i>Daphnia pulex</i>	400	73	7e-111	68
24	AY588067	Putative delta-9 desaturase	<i>Homalodisca coagulata</i>	596	31	6e-166	74
25	XP_003699739	tRNA-methyltransferase-like	<i>Megachile rotundata</i>	191	99	5e-54	46
26	XP_001948117	UDP-glucuronosyltransferase	<i>Acyrtosiphon pisum</i>	166	73	1e-45	51
27	YP_001310867	Formate dehydrogenase accessory protein	<i>Clostridium beijerinckii</i>	37.7	21	0.83	35
28	AD182776	Fatty-acyl CoA reductase 3	<i>Ostrinia nubilalis</i>	77.4	11	2e-12	72
29	XP_001842626	Conserved hypothetical protein	<i>Culex quinquefasciatus</i>	104	19	3e-24	62
30	XP_003694962	Uncharacterized protein LOC100866274	<i>Apis florea</i>	172	13	1e-41	91
31	XP_974477	Similar to selenoprotein T	<i>Tribolium castaneum</i>	233	91	7e-74	52
32	XP_001651772	Swiprosin	<i>Aedes aegypti</i>	238	48	9e-59	72
33	NP_001156153	Superoxide dismutase [Cu-Zn]-like	<i>Acyrtosiphon pisum</i>	211	38	9e-63	65
34	AAD09820	Sarcoplasmic reticulum-type calcium ATPase	<i>Heliothis virescens</i>	942	82	0	88
35	XP_001943129	Calcium-transporting ATPase sarcoplasmic	<i>Acyrtosiphon pisum</i>	202	57	6e-57	87
36	XP_974142	Similar to synaptic vesicle protein	<i>Tribolium castaneum</i>	172	34	9e-45	66
37	XP_001603603	PQ-loop repeat-containing protein 3-like	<i>Nasonia vitripennis</i>	167	62	3e-47	55
38	XP_001663157	Atlastin	<i>Aedes aegypti</i>	345	65	2e-110	67
39	XP_002425619	T-complex protein 1 subunit theta, putative	<i>Pediculus humanus corporis</i>	451	76	4e-133	76
40	XP_001950086	F-box/LRR-repeat protein 7-like	<i>Acyrtosiphon pisum</i>	54.7	12	3e-06	96
41	EF203751	Nascent polypeptide (NAC domain)	<i>Metarhizium anisopliae</i>	126	79	2e-33	77
42	EFN86788	Breast cancer type 1 susceptibility protein-like	<i>Harpegnathos saltator</i>	36.2	34	8.1	32
43	XP_001944192	Protein abrupt-like	<i>Acyrtosiphon pisum</i>	113	16	3e-25	73
44	AGJ26478	Vitellogenin	<i>Laodelphax striatellus</i>	664	99	0	99
45	EFN62397	High affinity copper uptake protein 1	<i>Camponotus floridanus</i>	126	12	9e-30	64
46	XP_001849608	Sugar transporter	<i>Culex quinquefasciatus</i>	147	63	4e-36	35
47	XP_003701206	Proton-coupled folate transporter-like	<i>Megachile rotundata</i>	106	48	5e-15	68
48	JAA63857	Prolow-density lipoprotein receptor	<i>Rhipicephalus pulchellus</i>	87.4	41	1e-15	39
49	AB549999	Sugar transporter 6	<i>Nilaparvata lugens</i>	1,491	95	0	86
50	KC632400	Ribosome associated membrane protein	<i>Coptotermes formosanus</i>	140	78	8e-30	78
51	EFN84609	Centromeric protein E	<i>Harpegnathos saltator</i>	38.5	17	4.9	36
52	XP_001947300	Probable G-protein coupled receptor	<i>Acyrtosiphon pisum</i>	404	86	6e-97	63
53	XP_003399831	Protein jagunal-like	<i>Bombus terrestris</i>	276	76	1e-90	71
54	NP_001037544	Transmembrane BAX inhibitor motif	<i>Bombyx mori</i>	87	31	1e-17	59
55	XP_002427607	Tetraspanin-18, putative	<i>Pediculus humanus corporis</i>	107	17	5e-23	55
56	AAB72002	JR-1	<i>Riptortus clavatus</i>	41.6	53	0.058	25
57	XM_001849781	ATP synthase lipid binding protein	<i>Culex quinquefasciatus</i>	286	48	2e-73	87
58	ZP_02864690	Peptidase, M16 family	<i>Clostridium perfringens</i>	34.3	49	8.7	28
59	YP_002908631	Nonribosomal peptide synthase	<i>Burkholderia glumae</i>	37	30	2.4	35
60	XP_970655	Similar to peroxisomal membrane protein	<i>Tribolium castaneum</i>	219	73	3e-64	41
61	XP_003702072	Tyrosine-protein phosphatase non-receptor	<i>Megachile rotundata</i>	42.7	8	0.25	59
62	EFN86838	Casein kinase II subunit	<i>Harpegnathos saltator</i>	450	42	2e-127	86
63	EFR27272	Hypothetical protein AND_06142	<i>Anopheles darlingi</i>	238	77	1e-71	70
64	NP_001128673	Cathepsin L like protein precursor	<i>Bombyx mori</i>	40	12	0.29	70
65	XP_966698	Similar to pyruvate kinase isoform 1	<i>Tribolium castaneum</i>	200	36	2e-42	76
66	XP_002087481	GE17166	<i>Drosophila yakuba</i>	35.4	22	6.3	38

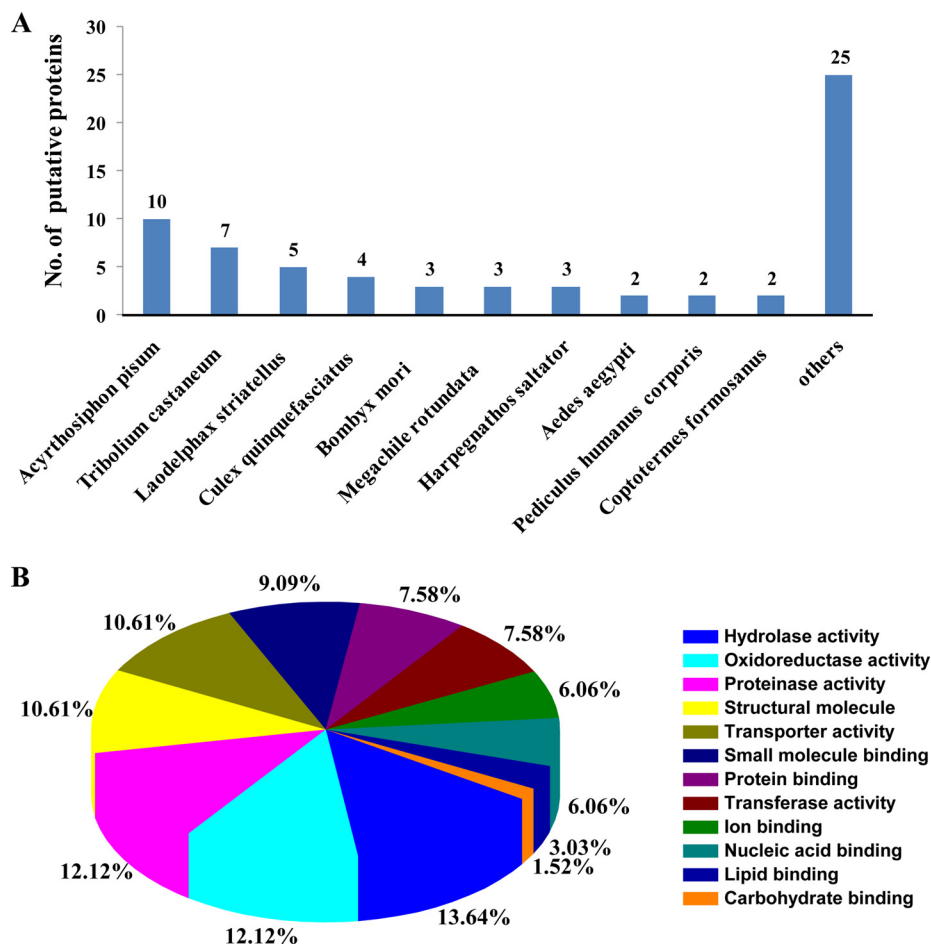


FIG. 1. Bioinformatics analysis of 66 proteins from *Laodelphax striatellus* that interacted with the nucleocapsid protein (pc3) of *Rice stripe virus* (RSV) in the yeast two-hybrid assay. (A) Species frequency distribution of 66 putative interactors. The number above each bar is the number of proteins matched from that species. (B) Distribution by molecular function of the screened proteins of *L. striatellus* from the yeast two-hybrid system. The GO classification identified 12 functional categories for the 66 putative interactors. Different colors represent different functional classes.

(13 times stronger than the control), atlastin (seven times the control), jagnual (six times the control), vitellogenin (five times the control), NAC domain protein (two times the control) (Fig. 3C). The protein with the strongest interaction with pc3, CPR1, was selected to for further study.

Amplification of Full-Length CPR1 and Bioinformatics Analysis—After sequencing the CPR1 plasmid from the screened yeast clone, we obtained nearly the full-length nucleotide sequence (1,722 bp) of CPR1. We then used 5'RACE to obtain the 5' untranslated region of 83 bp. The full-length cDNA of CPR1 was 1,805 bp long, contained a 648-bp open reading frame that encoded a 215-amino acid protein, an 83-bp 5' untranslated region, and a 1,074-bp 3' untranslated region (GenBank accession no. KC485263). CPR1 has a RR1 consensus (Rebers and Riddiford consensus), which is known to bind chitin (Figs. S3A and S3B) (38). It does not contain any transmembrane domain (Fig. S3C). When compared with 25 other insect cuticular proteins in the NJ tree analysis with the MEGA v. 5, CPR1 was not closely related to any of them (Fig.

S4), suggesting that it evolved independently or may be a new type of cuticular protein.

Analysis of Different Fragments in CPR1 That Interact with RSV pc3—To determine which fragments of CPR1 bind with RSV pc3, the protein was divided into two fragments: The chitin bind 4 domain (CPR1-N, 1aa-90aa) and an unknown function domain (CPR1-C, 91aa-215aa), and the full-length gene and two fragments of the gene, respectively, were amplified by PCR. The full length and two fragments were tested for any interaction with RSV pc3 using the yeast two hybrid and pull-down assays. The yeast two hybrid assay showed that CPR1 had a strong interaction with RSV pc3 and fragment CPR1N had a weak interaction with RSV pc3, but fragment CPR1C did not interact with RSV pc3 (Figs. 4A and 4B). The result from the pull-down assay was consistent with the yeast two hybrid assay. CPR1 and fragment CPR1N can interact with RSV pc3, fragment CPR1C cannot. The assay also showed that the interaction of CPR1 with RSV pc3 was stronger than CPR1N with RSV pc3 (Fig. 4C).

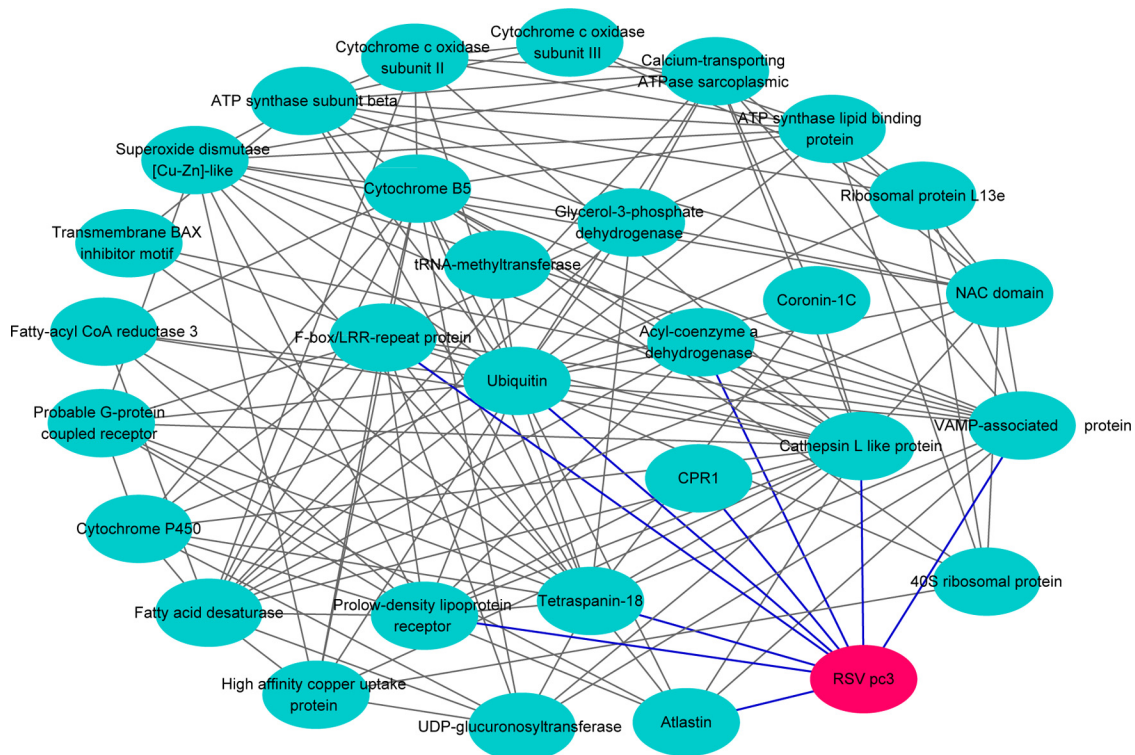


FIG. 2. Virus-insect protein interaction network analysis of RSV pc3 and *L. striatellus* homologs with *Drosophila melanogaster* was generated with Cytoscape.

Subcellular Colocalization of RSV pc3, RSV RNPs, and CPR1 in Cells of Sf9 or *L. striatellus*—Sf9 cells were coinoculated with recombinant baculovirus encoding pc3 and CPR1 then treated with RSV pc3 antibody labeled with Alexa Fluor 594 (red) and CPR1 antibody with Alexa Fluor 488 (green). Confocal fluorescence images revealed that the two proteins colocalized with each other in large, irregular structures (Fig. 5A). To discover whether CPR1 colocalizes with RSV RNPs, we used RSV to infect *L. striatellus* cells then treated these viruliferous cells with the fluorescence-labeled RSV and CPR1 antibodies. Confocal fluorescence images of these cells showed that CPR1 colocalized with RSV RNPs (Fig. 5B).

Colocalization of RSV RNPs and CPR1 in *L. striatellus*—After total RNA was extracted from dissected salivary gland, gut, ovary tissues, and hemolymph, we used real-time qRT-PCR to analyze 200 ng of RNA from each sample for relative expression of CPR1. The expression level of CPR1 from the same tissue did not obvious differ between viruliferous and nonviruliferous insects (Fig. 6A), indicating that virus did not affect CPR1 expression levels. However, among the various tissues, CPR1 was more highly expressed in the hemolymph and salivary gland than in the gut and ovary (Fig. 6A). To determine whether CPR1 colocalized with RSV RNPs in the *L. striatellus*, we used laser scanning confocal microscopy to detect the CPR1 and RSV RNPs in various tissues and hemocytes. In the salivary gland and ovary, only the virus was

observed; the CPR1 was not (Figs. 6B and 6E). Considering the expression results of CPR1 in these tissues, CPR1 was present but not detectable with antibody. In the gut, CPR1 was primarily on the surface of the tissue, whereas RSV RNPs appear to be localized in the epithelial cells of the gut. Apparently then, they are in different locations (Fig. 6D). In the hemocytes isolated from the hemolymph, both RSV RNPs and CPR1 were visualized, so they can colocalize in these cells (Fig. 6C). Thus, the site of CPR1 and virus binding *in vivo* may be in the hemolymph of *L. striatellus*.

Interference of CPR1 Expression Led to a Decrease in RSV Titer and Transmission Efficiency—To clarify whether CPR1 affects virus movement in the insect vector, RNA interference (RNAi) technology and microinjection of third-instar viruliferous nymphs were used to knock down the expression of CPR1 in the *L. striatellus*. After microinjection with CPR1 dsRNA (dsCPR1) or GFP dsRNA (dsGFP) (control), the real-time qRT-PCR was used to test the expression levels of CPR1 and virus in the hemolymph, salivary glands, and gut of the insects. CPR1 mRNA levels in the dsCPR1-injected insects were significantly lower than in the control group from the hemolymph and tested tissues at all times, with the lowest levels (>90% reduction) recorded at 2 days post injection (Figs. 7A-7C). The mRNA levels of RSV pc3 in the dsCPR1-injected insect decreased significantly in the hemolymph and salivary gland, but not in the gut tissue (Figs. 7D-7F). Levels were significantly reduced by 4 days in the hemolymph and by

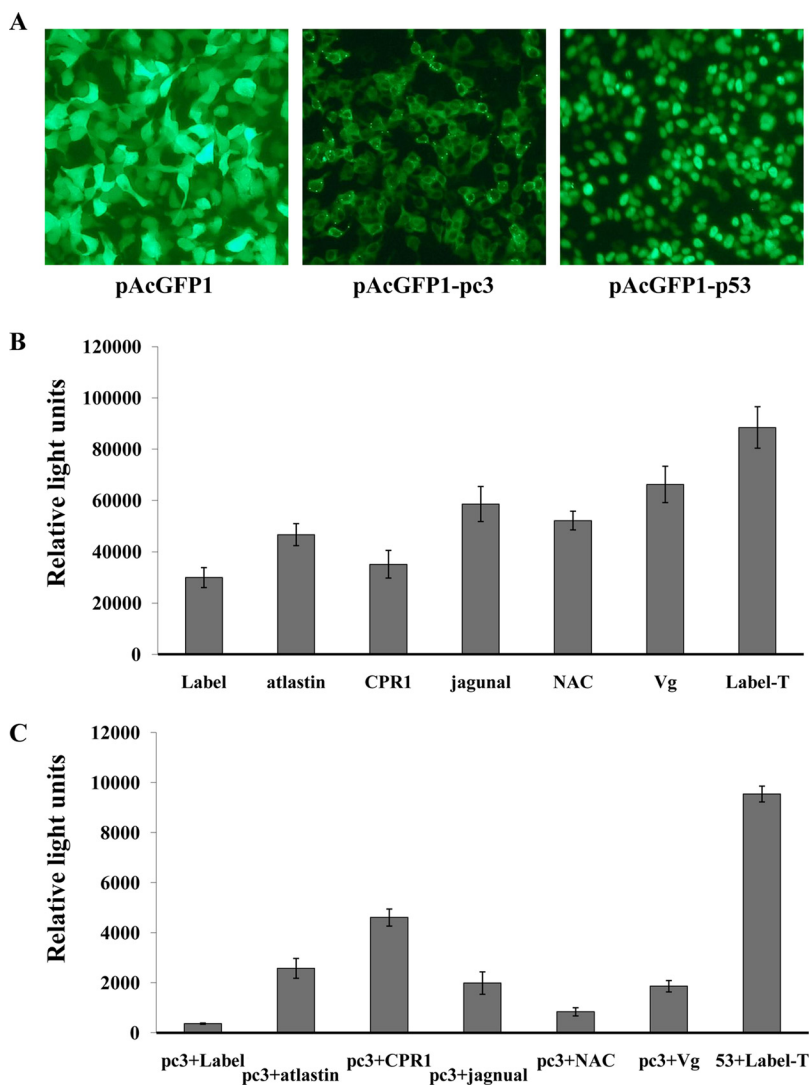


FIG. 3. Confirmed interaction between RSV pc3 and proteins of *L. striatellus* using chemiluminescent co-immunoprecipitation. (A) AcGFP1-pc3 fusion protein in HEK 293FT cells detected using fluorescence microscopy. (B) Five prey proteins fused with Prolabel were detected expression from HEK 293FT cells. (C) Confirmed interaction between RSV pc3 and 5 prey proteins by chemiluminescent co-immunoprecipitation. Recombinant plasmids of pAcGFP1-pc3 and pProlabel-atlastin, pProlabel-CPR1, pProlabel-jagunal, pProlabel-NAC or pProlabel-Vg (vitellogenin) were used to co-transfect 293FT cells. Interactions between RSV pc3 and prey protein were detected together with positive (GFP1-53 and Label-T) and negative controls (GFP1-pc3 and Label). Relative light units for ProLabel activity represent the strength of the interaction between the two proteins.

6 days in the salivary gland (Figs. 7D and 7E). The transmission efficiencies of insects with injected dsCPR1 and dsGFP was 21 and 49%, respectively. Viral transmission efficiency was also significantly lower for the dsCPR1-injected insects than for the control group (Fig. 7G). Different tissues (salivary glands, gut and hemocyte) of the injected insects were also excised and viewed with confocal microscopy. The dsCPR1-treated insecta did not differ visually from the control insects (Fig. S5). All these data suggested that the decreased level of CPR1 in the insects led to an associated decrease in the virus levels in the hemolymph and entering the salivary glands.

DISCUSSION

Movement of the virus through different organs in the vector insect requires specific interactions between components of the virus and the insect vector (3, 6). The yeast two-hybrid system, widely used in proteomics research of uncharacterized protein-protein interactions, is also conducive to the study of insect proteins involved in viral transmission (16). Our study focused on RSV pc3, the nucleocapsid protein, which plays an essential role in the retention or movement of the virus in the insect vector and is a determinant for viral transmission by the insect (39-41). So the insect proteins that interact with RSV pc3 may facilitate virus movement or sur-

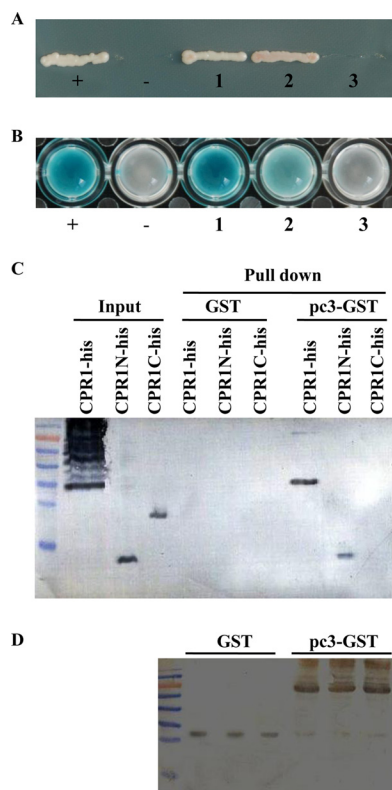


FIG. 4. Analysis of interaction between RSV pc3 and CPR1, CPR1N, CPR1C. (A) CPR1, CPR1N, and CPR1C were used with RSV pc3 to cotransform yeast for growth on quadruple dropout medium (SD/-Leu /-Trp/-His/-Ade) selective medium. The CPR1, CPR1N, or CPR1C gene was inserted into prey plasmid pPR3N, and RSV pc3 was inserted into the bait plasmid pDHB1. The recombinant plasmids were used to cotransform yeast. (+: positive control, -: negative control, 1: pc3+ CPR1, 2: pc3+CPR1N, 3: pc3+CPR1C). (B) The yeast clones that contained different plasmids were detected in a β -galactosidase activity assay. CPR1 and CPR1N interacted with RSV pc3, but CPR1C did not interact with RSV pc3. (+: positive control, -: negative control, 1: pc3+ CPR1, 2: pc3+CPR1N, 3: pc3+CPR1C). (C) The GST pull-down assay was used to detect an interaction between RSV pc3 and different CPR1 fragments. RSV pc3 was fused with GST to act as a bait protein with a single GST as a control. CPR1 and CPR1N interacted with RSV pc3, but CPR1C did not interact with RSV pc3. None of them interacted with GST (negative control). (D) Pull-down samples were detected with GST antibody to ensure equal sample loading.

vival in the insect vector. Thus, the RSV pc3 as a bait protein was used to screen the cDNA library of insect vector *L. striatellus*, and 66 interacting proteins were identified (Table I). These screened proteins were classified among 12 molecular function categories. Of these proteins, only 29 proteins were found to be homologous with proteins in *D. melanogaster* and were then used to construct a protein interaction network with RSV pc3. Because *L. striatellus* is a hemipteran, it is quite different from the dipteran *D. melanogaster*, and most of *L. striatellus*' proteins do not have matches in the flybase, and some matched proteins did not interact with RSV pc3 directly (Fig. 2). However, the network still illustrated that these pro-

teins may be involved in the complex interaction with others, perhaps to aid in overcoming different tissue barriers in *L. striatellus* to enable the movement and subsequent transmission of RSV.

Based on the network and molecular function of the screened proteins, five proteins (atlastin, CPR1, jagunal, NAC, and vitellogenin) were selected to confirm interaction with RSV pc3 using the chemiluminescent Co-IP assay (Fig. 3). Atlastin as a GTPase, which localizes to the endoplasmic reticulum (ER), is essential for homotypic membrane fusion of ER membranes (42, 43). The ER, a continuous membrane system of interconnected tubules, pervades the cytoplasm in all eukaryotes and functions in protein translation, folding and transport (44). Because studies have shown that plant viruses such as *Grapevine fanleaf virus* and *Brome mosaic virus* can replicate in the ER (45, 46), atlastin may aid RSV movement and/or replication in the cells of *L. striatellus*. The NAC domain protein was originally characterized as the first ribosome-associated protein to contact the emerging viral polypeptide chain (47). The NAC domain protein can also enhance replication of *Tomato leaf curl virus* by binding the viral replication accessory protein (48). Thus, we propose that NAC, found here to bind RSV pc3, may play an important role in viral replication. Previous studies showed that jagunal is required for reorganizing the ER during oocyte growth (49). We suggested that jagunal, which interacted with RSV pc3, may be involved in virus movement in the oocyte of *L. striatellus*. In our previous report, we showed evidence that Vg played a critical role in RSV entering the ovary of *L. striatellus* (15). Furthermore, several cuticular proteins of insects have been implicated in the transmission of other circulative plant viruses (50, 51). Thus, we speculated that CPR1, confirmed by Co-IP analysis to interact strongly with RSV pc3, may have an important role in virus transmission.

In a series of experiments, we further studied the function of CPR1 to find that it colocalized not only with RSV pc3 in the Sf9 cells, but also with RSV RNPs in cells of *L. striatellus* cells (Figs. 5A and 5B). This colocalization seems to indicate that CPR1 does indeed bind to pc3 and RNPs of RSV, suggesting that these specific protein-protein interactions determine the specificity between the virus and its vector.

Hundreds of cuticular proteins have been identified and analyzed in various insect species (52). These proteins and the polysaccharide chitin form the exo- and endocuticular layers that comprise the procuticle, which with the epicuticle makes up the insect exoskeleton (cuticle or integument), covering the entire body wall and the appendages as well as the foregut, hindgut, and tracheae as protection from microbial infection and physical and other environmental stresses (53). Most cuticular proteins are synthesized in the epidermal cells then transported to the cuticle, trachea, and other tissues via the hemolymph (54). Additionally, some cuticular proteins are synthesized by hemocytes that circulate in the hemolymph. A microarray analysis showed that mRNAs from hemocytes

Fig. 5. Subcellular colocalization of (A) CPR1 and RSV pc3 or (B) RSV RNPs in cells of *S. frugiperda* 9 Cells or *L. striatellus* cultured in monolayers. (A) CPR1 and RSV pc3 in Sf9 cells. CPR1 (Alexa Fluor 488, green) and RSV pc3 (Alexa Fluor 594, red) colocalized with each other in irregular patches in Sf9 cells (BF, bright field; bars, 5 μ m). (B) CPR1 and RSV RNPs in *L. striatellus* cells. CPR1 (Alexa Fluor 594, red) and RSV RNPs (Alexa Fluor 488, green) were localized in the viruliferous *L. striatellus* cells. They also colocalized with each other in the cells. Detailed view of boxed areas are indicated by arrows. (bars, 20 μ m).

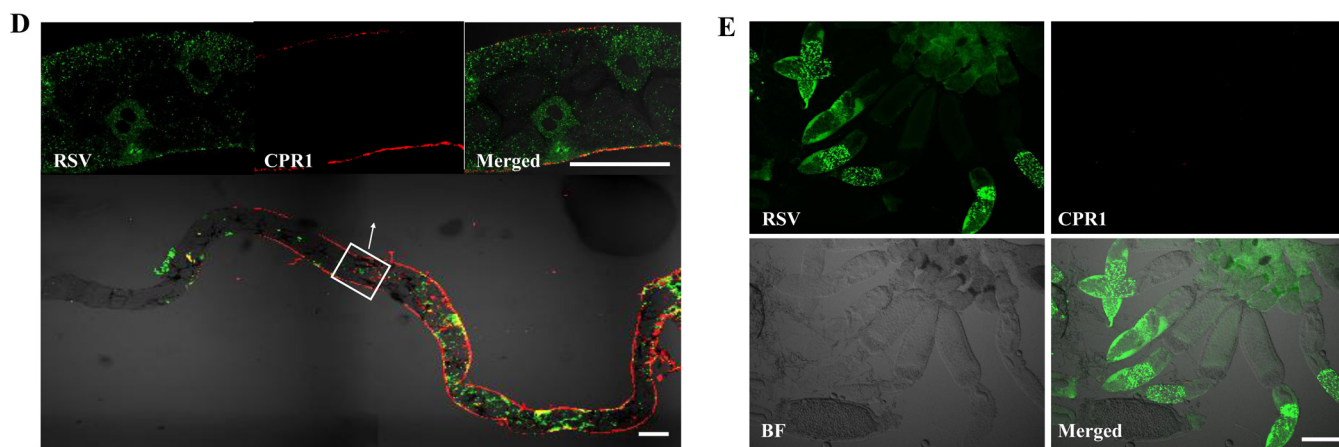
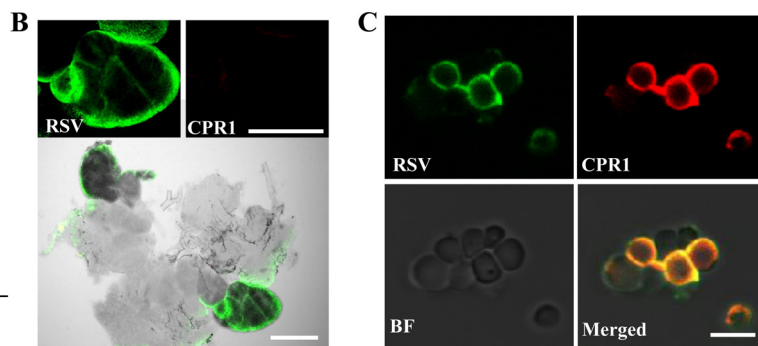
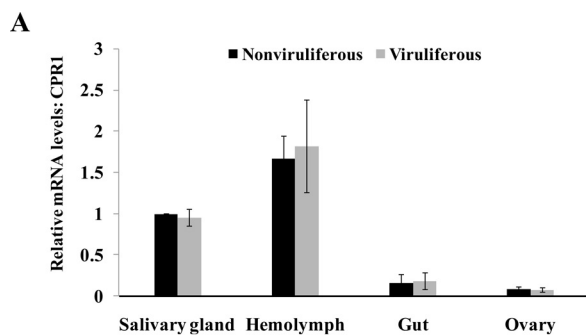
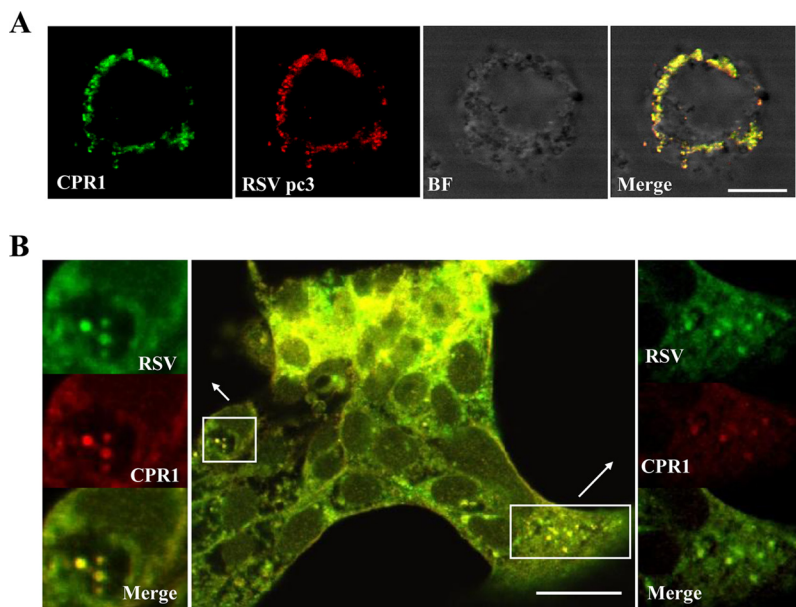


Fig. 6. Expression of CPR1 and colocalization of RSV RNPs and CPR1 in different tissues of *L. striatellus*. (A) Relative levels of CPR1 mRNA in excised salivary glands, hemolymph, gut, and ovary from viruliferous and nonviruliferous insects. The data represent means \pm standard deviations from three individual real-time qRT-PCR experiments, $*p < .01$. (B-E) Confocal micrographs of RSV RNPs and CPR1 colocalized in viruliferous, excised (B) salivary glands, (C) hemocytes, (D) gut, and (E) ovary and hemocytes were isolated and fixed on treated cover slips. In D the boxed area is enlarged in the merged image. Samples were stained with RSV antibody conjugated to Alexa Fluor 488 (green) and CPR1 antibody Alexa Fluor 594 (red) (B, E; bars, 100 μ m; C; bars, 10 μ m; D; bars, 50 μ m; BF, bright field).

isolated from *Anopheles gambiae* encoded nine cuticular proteins (54, 55). The majority of cuticular proteins have a 35–36 amino acid motif known as the Rebers and Riddiford consen-

sus (RR consensus) sequence, which is known to bind chitin (38). The RR sequence is the basis for dividing the cuticular proteins into three groups; the two main groups, RR-1 and

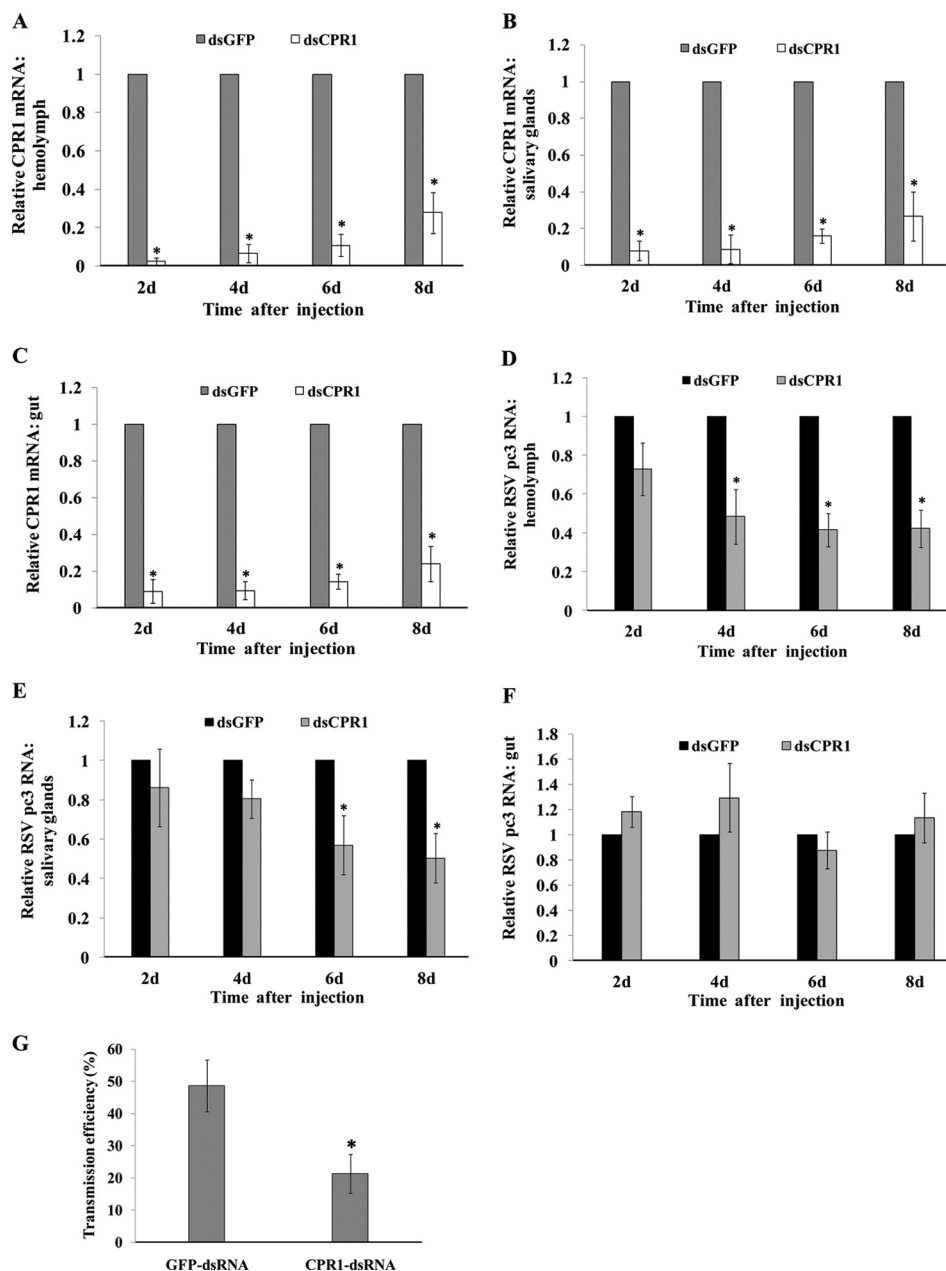


FIG. 7. Effect of CPR1 RNAi knockdown on *Rice stripe virus* (RSV) in hemolymph, salivary glands, and gut removed from viruliferous *L. striatellus* at various times after injection with CPR1 dsRNA (dsCPR1) or GFP dsRNA (dsGFP) (control). Real-time qRT-PCR was used to quantify the transcript level of (A-C) CPR1 or (D-F) RSV pc3 in tissues. (G) Efficiency of virus transmission in to rice seedlings by insects after injection. Control insects were injected with GFP dsRNA and infected 49% of the rice seedlings; the CPR1 dsRNA-injected insects infected 21%. The RNA level in the dsGFP group was designated as one. The results of qRT-PCR were normalized to the internal control gene, actin. Error bars represent means \pm standard deviations from three individual experiments, * $p < .01$).

RR-2, are found in most insects, but RR-3 has been identified only in a small number of insects (38, 56, 57). CPR1 belongs to the cuticular protein RR-1 group as determined using the Hidden Markov Model at the cuticleDB database (Fig. S3A) (58). The RR-1 cuticular proteins are mainly associated with the soft cuticle of many insects (38), suggesting that CPR1, which was highly expressed in the hemolymph and localized in the hemocytes, may be synthesized by the hemocytes of *L.*

striatellus (Figs. 6A and 6C) then moves to a particular tissue in the circulating hemolymph. CPR1 and virus cannot colocalize in the gut of *L. striatellus* (Fig. 6D). Because RSV pc3 can only interact with fragment CPR1N, not fragment CPR1C (Fig. 4), we speculated that CPR1, which contains the chitin binding 4 domain (CPRN), might become modified in the gut by binding to chitin or other proteins (Fig. S3B). Thus, it led to the virus cannot bind to CPR1 in the gut.

Previous studies showed that several cuticular proteins, with molecular masses between 22 and 31 kDa, are located in the stylets of the green peach aphid, *Myzus persicae*, and might interact with the helper component-proteinase of *Zucchini yellow mosaic virus* (1, 51). At least four cuticular proteins have also been proposed to be involved in the transmission process of the persistent *Cereal yellow dwarf virus-RPV* by its aphid vector (*Schizaphis graminum*) (50). Although many cuticular proteins have been implicated in plant virus transmission by an insect, their function in the transmission process has been unknown. Our present work provides the first direct experimental evidence that the cuticular protein CPR1 and virus can bind to each other in the hemocytes (Fig. 6C). Inhibition of CPR1 expression led to a decrease in virus levels in the hemolymph (Fig. 7D), which functions in immune reactions against invading macromolecules in different insect species (59). A virus can be considered as a type of invading “macromolecule,” but one that could evolve special mechanisms against an insect’s immune responses (60). Symbionin, a GroEL homolog protein that is produced by a symbiotic bacterium of insects and released into the hemolymph, has been shown to interact with a plant virus *in vitro* (20). The protein has been proposed to protect the virus from destruction in the hemolymph. The main evidence for the role of GroEL in *Barley yellow dwarf virus* transmission is that it can bind to the viral readthrough domain *in vitro* (20). However, in a recent report, GroEL did not interact with *Barley yellow dwarf virus* particles *in vivo* and was not detected in the aphid hemolymph, fat body, or gut, suggesting that GroEL is unlikely to protect the virus in the hemolymph of aphids (21). Other mechanisms therefore seem more likely to be responsible for hemolymph transmission of a plant virus. The proteins from *L. striatellus* that we found to contribute to RSV transmission in the hemolymph have not even been reported yet. On the basis of our findings, the virus may escape immune attack in the hemolymph by binding to CPR1, a cuticular protein of the insect. In other words, CPR1 may somehow enable viral survival in the insect hemolymph.

Persistent, circulative, propagative plant viruses will further replicate in various organs, including the hemolymph of insects such as reoviruses in leafhoppers (2). As a persistent, circulative, propagative virus, RSV may also replicate in the hemolymph of *L. striatellus*. Thus, when the expression of CPR1 decreased, virus levels decreased in the hemolymph (Fig. 7D), indicating that the CPR1, in binding the virus in the hemocytes, might facilitate virus replication in the hemolymph. Our study also showed that inhibition of CPR1 expression led to a decrease in virus levels in the salivary glands (Fig. 7E). At the same time, the efficiency of virus transmission was also reduced in the dsCPR1-treated groups (Fig. 7G). However, CPR1 is not present in the salivary glands (Fig. 6B). These data suggested that the most likely effect of CPR1 on the amount of virus in the salivary glands may be indirect. The insect hemolymph, critical to the successful transmission of

insect vectors, can be used as a bridge to the salivary glands. It plays a vital role in transporting hormones, nutrients and wastes and in regulating chemical exchanges between tissues (61). We propose that the amount of virus in the hemolymph is reduced, and fewer viral particles are then transported to the salivary glands. Hence, CPR1 may bind to the virus in the hemolymph then assist virus movement into the salivary glands.

To summarize, we used the split-ubiquitin yeast two-hybrid system to obtain many insect proteins that interacted with RSV pc3. The proteins, representing a wide range of functional groups, could act at different stages in viral movement, replication, or overcoming transmission barriers in the insect vector. Four proteins of *L. striatellus* are speculated to be involved in viral transport, replication, and transovarial transmission. This work also provided evidence that the cuticular protein CPR1 is involved in the transmission process and is essential for RSV transmission in the insect vector. It might act at different points in the RSV life cycle, from protecting the virus or the replicating viral RNA from immune responses in the hemolymph and/or assisting the virus in moving into the salivary glands. All the evidence suggests that the virus can use existing proteins of the insect vector to enable its movement, replication, and survival in the hemolymph and eventually contributing to its transmission. Numerous viruses must circulate in their insect vectors, overcome insect defense responses, and protect themselves as they traverse the hemolymph. Thus, the identities of these putative vector proteins are of major importance and could lead to new disease control strategies.

Acknowledgments—We thank Professor Anna Whitfield (Kansas State University) for discussing and improving the English text. We gratefully acknowledge editorial assistance from Dr. Beth E. Hazen (Willows End, scientific editing and writing).

* This work was supported by the National Key Basic Research of China (2010CB126200), Natural Science Foundation of China (NSFC31401713), China Postdoctoral Science Foundation (2014M560145), and the Special Fund for Agro-scientific Research in the Public Interest (201303021). The funders had no role in study design, data collection and analysis, decision to publish, or preparation of the manuscript.

☐ This article contains supplemental material Table S1 and Figs. S1-S5.

** To whom correspondence should be addressed: State Key Laboratory for Biology of Plant Diseases and Insect Pests, Institute of Plant Protection, Chinese Academy of Agricultural Sciences, Beijing 100193, China. Tel: 8610-62815928, Fax: 8610-62815609. E-mail: xfwang@ippcaas.cn, wangxifeng@caas.cn.

REFERENCES

1. Uzest, M., Gargani, D., Drucker, M., Hébrard, E., Garzo, E., Candresse, T., Fereres, A., and Blanc, S. (2007) A protein key to plant virus transmission at the tip of the insect vector stylet. *Proc. Natl. Acad. Sci. U.S.A.* **104**, 17959–17964
2. Hohn, T. (2007) Plant virus transmission from the insect point of view. *Proc. Natl. Acad. Sci. U.S.A.* **104**, 17905–17906
3. Hogenhout, S. A., Ammar el, D., Whitfield, A. E., and Redinbaugh, M. G.

- (2008) Insect vector interactions with persistently transmitted viruses. *Annu. Rev. Phytopathol.* **46**, 327–359
4. Gray, S. M., and Banerjee, N. (1999) Mechanisms of arthropod transmission of plant and animal viruses. *Microbiol. Mol. Biol. Rev.* **63**, 128–148
 5. Sylvester, E. S. (1980) Circulative and propagative virus transmission by aphids. *Annu. Rev. Entomol.* **25**, 257–286
 6. Power, A. G. (2000) Insect transmission of plant viruses: a constraint on virus variability. *Curr. Opin. Plant Biol.* **3**, 336–340
 7. Schwarz, A., Tenzer, S., Hackenberg, M., Erhart, J., Gerhold-Ay, A., Mazur, J., Kuharev, J., Ribeiro, J. M., and Kotsyfakis, M. (2014) A systems level analysis reveals transcriptomic and proteomic complexity in *Ixodes ricinus* midgut and salivary glands during early attachment and feeding. *Mol. Cell. Proteomics*
 8. Gray, S., and Gildow, F. E. (2003) Luteovirus-aphid interactions. *Annu. Rev. Phytopathol.* **41**, 539–566
 9. Whitfield, A. E., Ullman, D. E., and German, T. L. (2005) Tospovirus-thrips interactions. *Annu. Rev. Phytopathol.* **43**, 459–489
 10. Wang, X., and Zhou, G. (2003) Identification of a protein associated with circulative transmission of barley yellow dwarf virus from cereal aphids, *Schizaphis graminum* and *Sitobion avenae*. *Chinese Sci. Bull.* **48**, 2083–2087
 11. Seddas, P., Boissinot, S., Strub, J. M., Van Dorsseleer, A., Van Regenmortel, M. H., and Pattus, F. (2004) Rack-1, GAPDH3, and actin: Proteins of *Myzus persicae* potentially involved in the transcytosis of beet western yellows virus particles in the aphid. *Virology* **325**, 399–412
 12. Li, C., Cox-Foster, D., Gray, S. M., and Gildow, F. (2001) Vector specificity of barley yellow dwarf virus (BYDV) transmission: Identification of potential cellular receptors binding BYDV-MAV in the aphid, *Sitobion avenae*. *Virology* **286**, 125–133
 13. Bandla, M. D., Campbell, L. R., Ullman, D. E., and Sherwood, J. L. (1998) Interaction of tomato spotted wilt tospovirus (TSWV) glycoproteins with a thrips midgut protein, a potential cellular receptor for TSWV. *Phytopathology* **88**, 98–104
 14. Tamborindeguy, C., Bereman, M. S., DeBlasio, S., Igwe, D., Smith, D. M., White, F., MacCoss, M. J., Gray, S. M., and Cilia, M. (2013) Genomic and proteomic analysis of *Schizaphis graminum* reveals cyclophilin proteins are involved in the transmission of cereal yellow dwarf virus. *Plos One* **8**, e71620
 15. Huo, Y., Liu, W., Zhang, F., Chen, X., Li, L., Liu, Q., Zhou, Y., Wei, T., Fang, R., and Wang, X. (2014) Transovarial transmission of a plant virus is mediated by vitellogenin of its insect vector. *PLoS Pathog.* **10**, e1003949
 16. Mar, T., Liu, W., and Wang, X. (2014) Proteomic analysis of interaction between P7-1 of southern rice black-streaked dwarf virus and the insect vector reveals diverse insect proteins involved in successful transmission. *J. Proteomics* **102**, 83–97
 17. Lavine, M. D., and Strand, M. R. (2001) Surface characteristics of foreign targets that elicit an encapsulation response by the moth *Pseudoplusia includens*. *J. Insect Physiol.* **47**, 965–974
 18. Lavine, M. D., and Strand, M. R. (2002) Insect hemocytes and their role in immunity. *Insect Biochemistry Mol.* **32**, 1295–1309
 19. Marmaras, V. J., and Lampropoulou, M. (2009) Regulators and signalling in insect haemocyte immunity. *Cellular Signalling* **21**, 186–195
 20. van den Heuvel, J. F., Bruyère, A., Hogenhout, S. A., Ziegler-Graff, V., Brault, V., Verbeek, M., van der Wilk, F., and Richards, K. (1997) The N-terminal region of the luteovirus readthrough domain determines virus binding to Buchnera GroEL and is essential for virus persistence in the aphid. *J. Virol.* **71**, 7258–7265
 21. Bouvaine, S., Boonham, N., and Douglas, A. E. (2011) Interactions between a luteovirus and the GroEL chaperonin protein of the symbiotic bacterium *Buchnera aphidicola* of aphids. *J. Gen. Virol.* **92**, 1467–1474
 22. Toriyama, S. (1986) Rice stripe virus: Prototype of a new group of viruses that replicate in plants and insects. *Microbiol. Sci.* **3**, 347–351
 23. Falk, B. W., and Tsai, J. H. (1998) Biology and molecular biology of viruses in the genus *Tenuivirus*. *Annu. Rev. Phytopathol.* **36**, 139–163
 24. Hibino, H. (1996) Biology and epidemiology of rice viruses. *Annu. Rev. Phytopathol.* **34**, 249–274
 25. Zhang, S., Li, L., Wang, X., and Zhou, G. (2007) Transmission of Rice stripe virus acquired from frozen infected leaves by the small brown planthopper (*Laodelphax striatellus* Fallén). *J. Virol. Methods* **146**, 359–362
 26. Franceschini, A., Szklarczyk, D., Frankild, S., Kuhn, M., Simonovic, M., Roth, A., Lin, J., Minguez, P., Bork, P., von Mering, C., and Jensen, L. J. (2013) STRING v9.1: Protein–protein interaction networks, with increased coverage and integration. *Nucleic Acids Res.* **41**, D808–D815
 27. Spinelli, S., Campanacci, V., Blangy, S., Moineau, S., Tegoni, M., and Cambillau, C. (2006) Modular structure of the receptor binding proteins of *Lactococcus lactis* phages. The RBP structure of the temperate phage TP901–1. *J. Biol. Chem.* **281**, 14256–14262
 28. Edgar, R. C. (2004) MUSCLE: Multiple sequence alignment with high accuracy and high throughput. *Nucleic Acids Res.* **32**, 1792–1797
 29. Morrison, D. A. (2006) Multiple sequence alignment for phylogenetic purposes. *Aust. Syst. Botany* **19**, 479–539
 30. Tamura, K., Peterson, D., Peterson, N., Stecher, G., Nei, M., and Kumar, S. (2011) MEGA5: Molecular evolutionary genetics analysis using maximum likelihood, evolutionary distance, and maximum parsimony methods. *Mol. Biol. Evol.* **28**, 2731–2739
 31. Felsenstein, J. (1985) Confidence limits on phylogenies: An approach using the bootstrap. *Evolution* **39**, 783–791
 32. Ma, Y., Wu, W., Chen, H., Liu, Q., Jia, D., Mao, Q., Chen, Q., Wu, Z., and Wei, T. (2013) An insect cell line derived from the small brown planthopper supports replication of *Rice stripe virus*, a tenuivirus. *J. Gen. Virol.* **94**, 1421–1425
 33. Marcellini, L., Giammatteo, M., Aimola, P., and Mangoni, M. L. (2010) Fluorescence and electron microscopy methods for exploring antimicrobial peptides mode(s) of action. *Meth. Mol. Biol.* **618**, 249–266
 34. Liu, S., Bonning, B. C., and Allen Miller, W. (2006) A simple wax-embedding method for isolation of aphid hemolymph for detection of luteoviruses in the hemocoel. *J. Virol. Meth.* **132**, 174–180
 35. Wang, Y., Mao, Q., Liu, W., Mar, T., Wei, T., Liu, Y., and Wang, X. (2014) Localization and distribution of *Wheat dwarf virus* in its vector leafhopper, *Psammotettix alienus*. *Phytopathology* **104**, 897–904
 36. Liu, S. H., Ding, Z. P., Zhang, C. W., Yang, B. J., and Liu, Z. W. (2010) Gene knockdown by intro-thoracic injection of double-stranded RNA in the brown planthopper, *Nilaparvata lugens*. *Insect Biochem. Mol.* **40**, 666–671
 37. Zhang, X., Wang, X., and Zhou, G. (2008) A one-step real time RT-PCR assay for quantifying rice stripe virus in rice and in the small brown planthopper (*Laodelphax striatellus* Fallén). *J. Virol. Meth.* **151**, 181–187
 38. Rebers, J. E., and Willis, J. H. (2001) A conserved domain in arthropod cuticular proteins binds chitin. *Insect Biochem. Mol.* **31**, 1083–1093
 39. Raccach, B., and Fereres, A. (2001) Plant virus transmission by insects. *eLS*, John Wiley & Sons, Ltd.
 40. Ziegler-Graff, V., and Brault, V. (2008) Role of vector-transmission proteins. *Methods Mol. Biol.* **451**, 81–96
 41. Bragard, C., Caciagli, P., Lemaire, O., Lopez-Moya, J. J., MacFarlane, S., Peters, D., Susi, P., and Torrance, L. (2013) Status and prospects of plant virus control through interference with vector transmission. *Annu. Rev. Phytopathol.* **51**, 177–201
 42. Bian, X., Klemm, R. W., Liu, T. Y., Zhang, M., Sun, S., Sui, X., Liu, X., Rapoport, T. A., and Hu, J. (2011) Structures of the atlastin GTPase provide insight into homotypic fusion of endoplasmic reticulum membranes. *Proc. Natl. Acad. Sci. U.S.A.* **108**, 3976–3981
 43. Orso, G., Pendin, D., Liu, S., Toso, J., Moss, T. J., Faust, J. E., Micaroni, M., Egorova, A., Martinuzzi, A., McNew, J. A., and Daga, A. (2009) Homotypic fusion of ER membranes requires the dynamin-like GTPase Atlastin. *Nature* **460**, 978–983
 44. Shimizu, Y., and Hendershot, L. M. (2007) Organization of the functions and components of the endoplasmic reticulum. *Adv. Exp. Med. Biol.* **594**, 37–46
 45. Ritzenthaler, C., Laporte, C., Gaire, F., Dunoyer, P., Schmitt, C., Duval, S., Piéquet, A., Loudes, A. M., Rohfritsch, O., Stussi-Garaud, C., and Pfeiffer, P. (2002) Grapevine fanleaf virus replication occurs on endoplasmic reticulum-derived membranes. *J. Virol.* **76**, 8808–8819
 46. den Boon, J. A., Chen, J., and Ahlquist, P. (2001) Identification of sequences in bromo mosaic virus replicase protein 1a that mediate association with endoplasmic reticulum membranes. *J. Virol.* **75**, 12370–12381
 47. Spreter, T., Pech, M., and Beatrix, B. (2005) The crystal structure of archaeal nascent polypeptide-associated complex (NAC) reveals a unique fold and the presence of a ubiquitin-associated domain. *J. Biol. Chem.* **280**, 15849–15854
 48. Selth, L. A. (2005) A NAC domain protein interacts with tomato leaf curl virus replication accessory protein and enhances viral replication. *Plant*

- Cell Online* **17**, 311–325
49. Lee, S., and Cooley, L. (2007) Jagunal is required for reorganizing the endoplasmic reticulum during *Drosophila* oogenesis. *J. Cell Biol.* **176**, 941–952
50. Cilia, M., Tamborindeguy, C., Fish, T., Howe, K., Thannhauser, T. W., and Gray, S. (2011) Genetics coupled to quantitative intact proteomics links heritable aphid and endosymbiont protein expression to circulative polerovirus transmission. *J. Virol.* **85**, 2148–2166
51. Dombrovsky, A., Gollop, N., Chen, S., Chejanovsky, N., and Raccah, B. (2007) In vitro association between the helper component-proteinase of zucchini yellow mosaic virus and cuticle proteins of *Myzus persicae*. *J. Gen. Virol.* **88**, 1602–1610
52. Karouzou, M. V., Spyropoulos, Y., Iconomidou, V. A., Cornman, R. S., Hamdrakas, S. J., and Willis, J. H. (2007) *Drosophila* cuticular proteins with the R&R Consensus: Annotation and classification with a new tool for discriminating RR-1 and RR-2 sequences. *Insect Biochem. Mol. Biol.* **37**, 754–760
53. Arakane, Y., Muthukrishnan, S., Beeman, R. W., Kanost, M. R., and Kramer, K. J. (2005) Laccase 2 is the phenoloxidase gene required for beetle cuticle tanning. *Proc. Natl. Acad. Sci. U.S.A.* **102**, 11337–11342
54. Gilbert, L. I. (2012) *Insect molecular biology and biochemistry*, 1st ed., Elsevier/Academic Press, London; Waltham, MA
55. Baton, L. A., Robertson, A., Warr, E., Strand, M. R., and Dimopoulos, G. (2009) Genome-wide transcriptomic profiling of *Anopheles gambiae* hemocytes reveals pathogen-specific signatures upon bacterial challenge and *Plasmodium berghei* infection. *BMC Genomics* **10**, 257–270
56. Togawa, T., Nakato, H., and Izumi, S. (2004) Analysis of the chitin recognition mechanism of cuticle proteins from the soft cuticle of the silkworm, *Bombyx mori*. *Insect Biochem. Mol. Biol.* **34**, 1059–1067
57. Cornman, R. S., Togawa, T., Dunn, W. A., He, N., Emmons, A. C., and Willis, J. H. (2008) Annotation and analysis of a large cuticular protein family with the R&R consensus in *Anopheles gambiae*. *BMC Genomics* **9**, 22–38
58. Cornman, R. S. (2009) Molecular evolution of *Drosophila* cuticular protein genes. *Plos One* **4**, e8345
59. Ribeiro, C., and Brehélin, M. (2006) Insect haemocytes: What type of cell is that? *J. Insect Physiol.* **52**, 417–429
60. King, J. G., and Hillyer, J. F. (2012) Infection-induced interaction between the mosquito circulatory and immune systems. *PLoS Pathog.* **8**, e1003058
61. Wyatt, G. R., and Pan, M. L. (1978) Insect plasma proteins. *Annu. Rev. Biochem.* **47**, 779–817